Proceedings of the 2nd Pacific International Conference on Application of Lasers and Optics 2006

<Edited by Milan Brandt and Erol Harvey>

EFFECT OF INCREMENT AND SINGLE-TRACK GEOMETRY ON THE FORMATION OF MULTI-TRACK LASER CLADDING

Shoujin Sun, Milan Brandt, James Harris, Yvonne Durandet

Industrial Laser Applications Laboratory, Industrial Research Institute Swinburne
Swinburne University of Technology, 533-545 Burwood Road, Hawthorn, Vic, 3122, Australia

Abstract

The variation of track geometry during multi-track laser cladding of stellite 6 on mild steel starting with different geometry profiles and levels of dilution in the single-track clad was examined. In transverse cross-section of the multi-track clad, the total area in each track includes the areas of melted powder (clad area), remelted previous track (remelted area) and melted substrate. Both clad area and total area increase with track number and finally reach constant values, but the increase of total area is much greater than that of clad area. The remelted area of previous track increases with the level of dilution of the single-track clad and reaches its maximum value when the dilution of single-track clad is over 20%. The percentage of the maximum remelted area of the previous track equals the percentage of the track overlap. The inter-track porosity will appear when the difference of the total area and the remelted area of the previous track is closer to or smaller than the clad area because there is not enough laser energy to melt the powder captured by the melt pool.

Introduction

In today's industry, the surface of many engineering components needs repairing after a period of service in order to extend their service life and working efficiency. Laser cladding is one of the techniques being used to repair and refurbish the damaged components because of its low heat input, low distortion of the workpiece and finer microstructure of the clad layer [1-6].

In the laser cladding process, laser energy melts the injected powder and fuses it to the substrate producing a fusion bond between the clad layer and substrate. The two most important features - clad height and dilution in single-track clad are controlled by laser power, powder mass flow rate, scan rate, types of powder and substrate materials [7, 8].

A single-track clad is performed with laser incident on the workpiece for one pass. The width of the track is smaller than or equal to the laser spot size and the clad height is dependent on the laser power, scan rate and powder mass flow rate [1-13]. In order to produce a clad layer with a required thickness and larger area coverage, the single-track clad has to be repeated and overlapped at a certain increment. The clad height and dilution of multi-track clad layer are significantly affected by this increment [13], which is an important process parameter especially when conducting the economic feasibility of the process.

Unlike the deposition of a single-track clad, the formation of a multi-track clad involves not only melting the injected powder, but also remelting part of the previous track, therefore the melted volume of substrate decreases which leads to the decrease of dilution. The whole area in one track of multi-track cladding includes the area contributed by melted powder, the area of remelted previous track and the melted substrate area.

The formation of multi-track clad has been examined. The amount of powder catchment in each track in multi-track cladding is assumed to be the same with that in the single-track cladding [14, 15]. This is true only for a large increment (larger than half of melt pool size). At small increment (smaller than half of melt pool size), the increase of both powder catchment and heat build-up makes the clad area and total area increase with track number. The variation of these areas with increment is important for formation of multi-track clad because an inappropriate increment could lead to a poor multi-track clad even though the single-track clad appears satisfactory (see Figure 1).

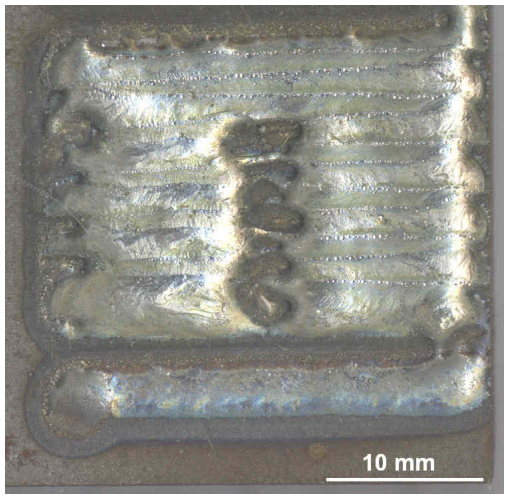

Figure 1. The appearance of multi-track clad with its single-track clad.

In the present study, the variation of these areas with track number at different increment is examined, and an empirical analysis model for the constant values of these areas is presented. A new criteria based on single-track clad geometry is proposed to judge whether and when an inter-track porosity occurs instead of the usual aspect ratio or ratio of clad height to increment.

Experimental procedure and empirical analysis

Laser cladding was carried out with a fibre delivered, high power Nd:YAG laser with a side injecting power nozzle. Laser beam was delivered by a 10m long step-index glass optical fiber with the diameter of 0.6mm. The cladding was performed with laser beam out of the focus plane, the different substrate/lens distance was set to give laser spot size ranging from 3 to 6mm at the surface of substrate.

Mild steel (300x75x10mm^3 in dimension) was chosen as the substrate, and stellite 6 was used as the clad powder. PSF, PSI and W grade powders (supplied by Stoody Deloro Stellite, Industry, CA.) with particle size ranging from <44, 44-74 and 149-231 micrometers (mesh 325/D, 200/325 and 180/100) respectively were used. Argon was used to deliver the powder and shield the melt pool.

The experiments were performed at different level of laser powers at workpiece (1200-2000W), scan rates (800-1600mm/min) and powder mass flow rates (13.5-28.5g/min) to achieve different geometry profiles of a single-track clad and its multi-track clad. The multi-track clad was made with the number of tracks varied from 1 to 14 at increments of 0.5, 1, 1.5 and 2mm respectively. The clad was then cross-sectioned, ground and polished to reveal its geometry. The clad area, total area, remelted area of previous track and substrate melted area in each clad were measured by using quantitative metallography. An empirical analysis model based on the quantitative metallography data was developed.

Results and discussion

Variation of clad geometry with track number

A transverse cross-section of a single-track clad with dilution of 36% is shown in Figure 2a. The bead does not show a symmetric profile probably due to the misalignment of powder jet and laser beam. Both the maximum height and depth of penetration appear at about 1/3 of the width of the bead instead of at 1/2 of the bead width.

The clad area (A_1^c) is defined as the area produced by the melted injected powder, which is the area above the substrate surface and the total area (A_1) is the overall melted area of the clad (the clad area A_1^c and the substrate penetrated area A_1^s). Both A_1^c and A_1 are determined by the characteristics of materials (powder and substrate) and laser processing parameters, such as power density, scan rate and powder mass flow.

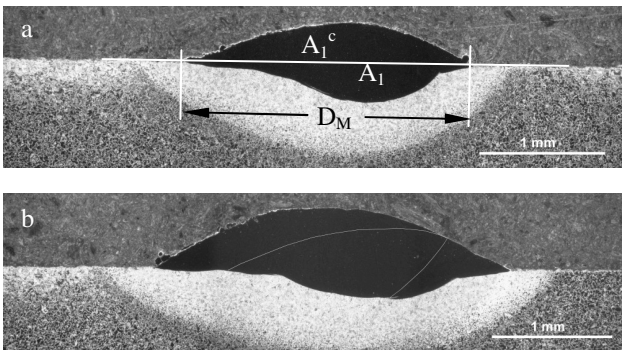

Figure 2. Transverse cross-section images of (a) a single-track and (b) a clad with 2 tracks.

In the multi-track cladding, a second clad track is deposited on the first clad track with an increment (Δx) in transverse direction. A new clad is partially laid on the top of the first clad track while part of the first clad track and substrate are melted as shown in Figure 2b. The total area in the second clad track (A_2) is composed of clad area (A_2^c), the remelted area of the first track clad (A_1^r) and the substrate penetrated area (A_2^s), i.e.:

$$A_2 = A_2^c + A_1^r + A_2^s \qquad (1)$$

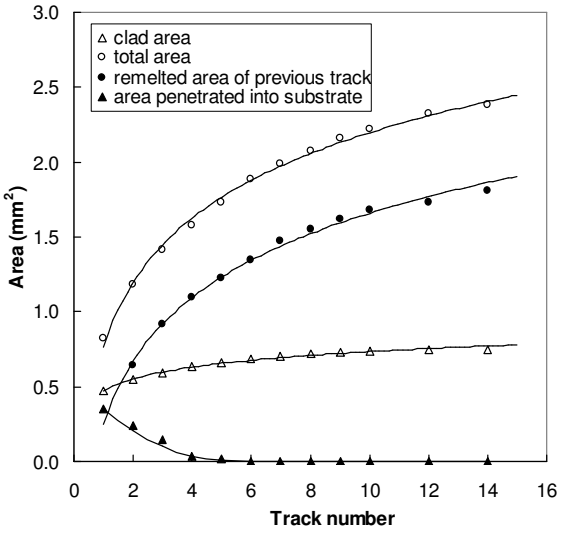

Figure 3. Variation of areas in each track with track number at the increment of 0.5mm.

The variation of these areas in each track for $\Delta x = 0.5\,\text{mm}$ is shown in Figure 3. Both total area (A_i) and remelted area of the previous track clad (A_{i-1}^r) in the i^{th} track increase dramatically with increasing track number, but the clad area A_i^c increases slightly and reaches a constant value at about track number $i = 12$. The A_i^s decreases with increasing track number and gets close to its constant value of 0 at about track number $i = 4$ which means that the dilution of 0% is achieved and an inter-track porosity is likely to be produced.

The effect of increment on the final values of clad area, total area and remelted area of the previous track clad is shown in Figure 4. Both A and A^r decrease dramatically, while A^c decreases slightly with increasing increment, the difference between A and A^r gets larger because of the smaller track overlap at larger increment. The substrate penetrated area A^s increases with increment, i.e. the A^s contributes more to the A at larger increment, therefore the dilution increases. Since these areas reach constant values, which determine the clad height, dilution and occurrence of inter-track porosity in the multi-track clad, empirical analysis of the steady values of these areas will be examined in the following sections.

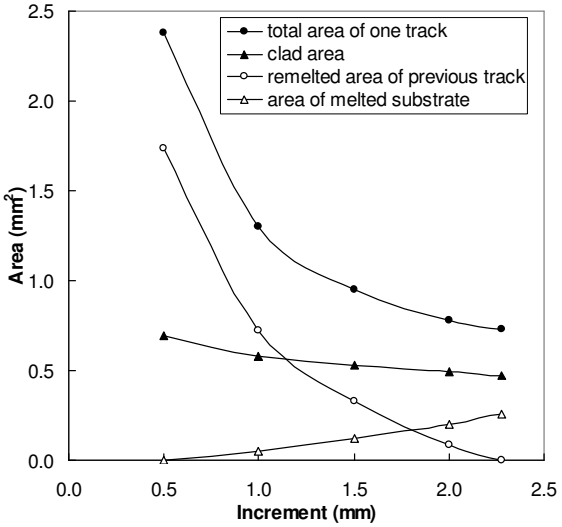

Figure 4. Effect of increment on the final areas of each track.

The empirical analysis of track geometry

Total Area, A A reason that the multi-track cladding is different from the single-track cladding is the heat build-up in the substrate and clad layer, which leads to an increase of total area in the subsequent track. The heat input is absorbed by injected powder, substrate and previous track. The heat is built up continuously in front of track until the balance between heat input and output is achieved. The total area made by one track reaches its maximum when the heat equilibrium is achieved. The steady value of total area in one clad track is found to depend on the increment and melt pool size (D_M), and can be expressed as follows:

$$\begin{cases} A = A_1 \cdot \left(\dfrac{D_M}{\Delta x}\right)^n & \text{when } 0 < \Delta x \le D_M \\ A = A_1 & \text{when } \Delta x > D_M \end{cases} \qquad (2)$$

where, n is a constant. The comparison between the experimental total area and calculated area by equation (2) is shown in Figure 5.

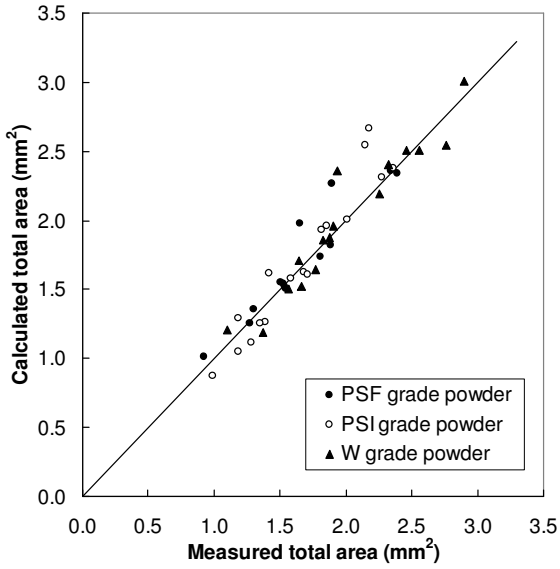

Figure 5. Correlation between the measured and calculated final value of total area.

It can be seen that the equation (2) can predict the total area well with n value of 0.77 for PSI and W grade powder and 0.55 for PSF grade powder respectively. The difference in n value between PSI and PSF powders is probably due to the difference in energy absorption between powders.

Remelted Area Of Previous Track, A^r_{i-1} The multi-track cladding not only melts the injected powder to form the clad but also melts the previous clad track to form good bonding between tracks. In the case of a single-track clad with dilution of 36%, the percentage of the ratio of A^r_{i-1} to the A_{i-1}, i.e., the percentage of the remelted area in one track by the following track is found to be constant and equal to the track overlap. The larger the track overlap (i.e., the smaller increment, or larger melt pool size), the more clad is remelted by the following track in the multi-track cladding. The relationship between the ratio of A_{i-1} to the A^r_{i-1} with track overlap can be written as:

$$\frac{A^r_{i-1}}{A_{i-1}} = k_r \cdot \frac{(D_M - \Delta x)}{D_M} \qquad \text{when } D_M > \Delta x > 0 \qquad (3)$$

where k_r is a coefficient dependent on the dilution (D) in the single-track clad as shown in Figure 6, which can be expresses as:

$$\begin{cases} k_r = 1 - 0.5 \times \dfrac{(0.2 - D)^{0.85}}{0.2} \cdot \exp\left(-\dfrac{D}{0.2 - D}\right) & \text{when } 0 < D < 20\% \\ k_r = 1 & \text{when } D \ge 20\% \end{cases} \qquad (4)$$

k_r is found only to be dependent on dilution and is independent of powder particle size.

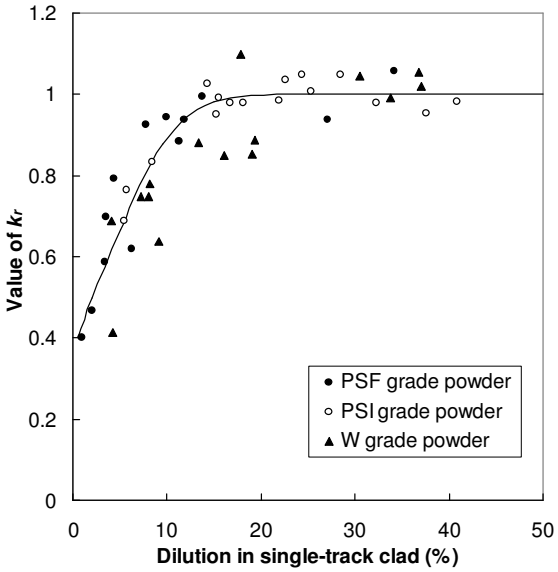

Figure 6. Effect of dilution in single-track clad on the k_r value.

The remelted area is determined by the dilution in a single-track clad and track overlap, and needs to be optimized to achieve good bonding between tracks.

Clad Area, A^c In addition to heat build-up, the change in laser beam incident angle with track build-up is another feature of multi-track cladding, which leads to increase in absorption and powder efficiency [16, 17]. This results in the increase of clad area (A_i^c) as shown in Figure 3. In the first track, the melt pool is normal to the laser beam in the transverse direction, the incident angle of laser beam in transverse direction is 0°. With increasing number of tracks, the incident angle increases, therefore, the melt pool size increases. Since only the powder falling into the melt pool is melted and forms a clad, the powder efficiency increases with the increasing melt pool size, i.e., the clad area (A^c) increases in multi-track clad as:

$$A^c = k_c \cdot A_1^c \qquad (5)$$

where k_c is the ratio of steady clad area in multi-track clad over the single-track clad. The k_c value is purely a function of the geometry of the melt pool and is found to increase with increasing track overlap, decreasing melt pool size and single track clad height ($h = \frac{A^c}{D_M}$) as:

$$\begin{cases} k_c = \left(\frac{D_M}{\Delta x}\right)^{\frac{D_L - D_M - \frac{h}{D_M}}{D_L}} & \text{when } 0 < \Delta x \le D_M \\ k_c = 1 & \text{when } \Delta x > D_M \end{cases} \qquad (6)$$

where D_L is the laser spot size. When the clad area in multi-track clad reaches its constant value, the clad height does not increase with number of tracks. Since there are $\frac{D_M}{\Delta x}$ tracks overlaid on one position, therefore, the average clad height of the multi-track clad (H) is the sum of $\frac{D_M}{\Delta x}$ single-track clad heights, i.e.:

$$H = \frac{D_M}{\Delta x} \cdot \frac{A^c}{D_M} = \frac{A^c}{\Delta x} = k_c \cdot \frac{A_1^c}{\Delta x} \qquad (7)$$

The comparison between the measured and calculated maximum clad height of multi-track clad is shown in Figure 7. The modification of clad area by k_c value makes the prediction of clad height more accurate.

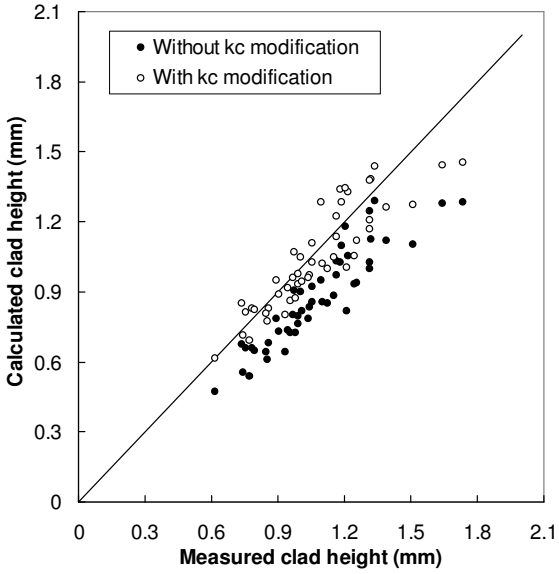

Figure 7. Comparison between the measured and calculated clad height with and without k_c modification.

Substrate Melted Area, A^s, Interface Bonding And Inter-track Porosity The substrate is melted by the laser energy after it is attenuated by the powder jet. The area of the melted substrate determines the dilution in multi-track clad. To make a fusion bond between the substrate and clad without loss of the superior wear resistance of stellite 6 clad, an appropriate level of dilution is require. Therefore, the substrate melted area A^s must be within a certain range. A^s can be calculated as follow:

$$A^s = A - A^r - A^c \qquad (8)$$

To achieve good bonding, $A^s > 0$ must be observed.

As discussed in the previous section, with increasing number of tracks, there is increasing percentage of injected powder captured by the enlarging melt pool, therefore, the laser energy attenuated through the powder jet decreases which leads to a reduction of substrate penetrated area in multi-track clad and the occurrence of the inter-track porosity.

Inter-track porosity is produced when the laser energy is not sufficient to melt the extra powder captured by the changing geometry of melt pool at the edge of previous track. The steeper the edge of the previous track, the more powder can be captured. Therefore, in this case, it is more likely to form the inter-track porosity. The criteria, the aspect ratio (the ratio of track width to clad height), or the ratio of clad height to the increment is normally used to determine whether the inter-track porosity occurs [1, 16].

However, a comparison of multi-track clad layers with same ratio of clad height to the increment (0.25) but different levels of dilution in the single-track clad in Figure 8 shows that the inter-track porosity occurs in the case of lower level of dilution in single-track clad (6%) but not in the multi-track clad with a higher level of dilution in the single-track clad (37%). Therefore, the occurrence of inter-track porosity depends not only on the ratio of clad height to the increment but also on the dilution in the single-track clad.

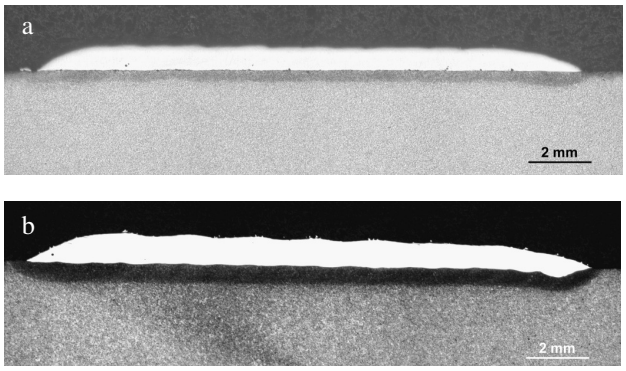

Figure 8. Occurrence of inter-track porosity in multi-track clad at dilution of (a) 6% in single-track clad and (b) 37% in single-track clad.

In order to make $A^s = 0$, the following condition must be observed:

$$A^c = A - A^r \qquad (9)$$

Therefore, we have the following criteria to eliminate the inter-track porosity by substituting equations (2), (3) and (5) in equation (9):

$$\begin{cases} k_e = \left(1 - k_r \cdot \dfrac{D_M - \Delta x}{D_M}\right) \cdot \left(\dfrac{D_M}{\Delta x}\right)^n \cdot \dfrac{A_l}{A_l^c} & \text{when } 0 < \Delta x \le D_M \\ k_e = \dfrac{A_l}{A_l^c} & \text{when } \Delta x > D_M \end{cases} \qquad (10)$$

In the case of single-track laser cladding with a given dilution, there is a proportion of laser energy that is attenuated through the powder jet to melt the substrate. With increasing k_c value, the proportion of laser energy that is attenuated decreases because of the capture of extra powder by the melt pool, therefore the substrate melted area decreases as described by equation (8).

k_e shows the limit of laser energy to melt the materials. When the k_c value gets close to or larger than the value of k_e, i.e. in the case of $k_c \ge k_e$, the laser energy is mostly absorbed by the powder, not enough penetration can be achieved. Therefore, the defects between tracks (inter-track porosity) and poor bonding between clad and substrate could be produced.

Taking the single-track clad with dilution of 36% in Figure 2 as an example, the values of k_e and k_c are calculated by using equations (10) and (6) and are plotted in Figure 9 as a function of increment. The k_e value increases while k_c value decreases with increasing increment. $k_c \ge k_e$ is observed in the case of both 0.5mm and 1mm increments. Therefore, the inter-track porosity appears at the 3rd and 7th track for 0.5 and 1.0 mm increments respectively as shown in Figure 10 (marked by the white arrows). No inter-track porosity has been found at 1.5 mm increment or larger since $k_c < k_e$ when increment is larger than 1mm. To get a good clad layer without inter-track porosity, the condition of $k_c < k_e$ must be observed.

The lower k_e value with finer powder while the k_c value is independent of powder particle size, as shown in Figure 9, can explain well the higher tendency for inter-track porosity formation with the finer powder.

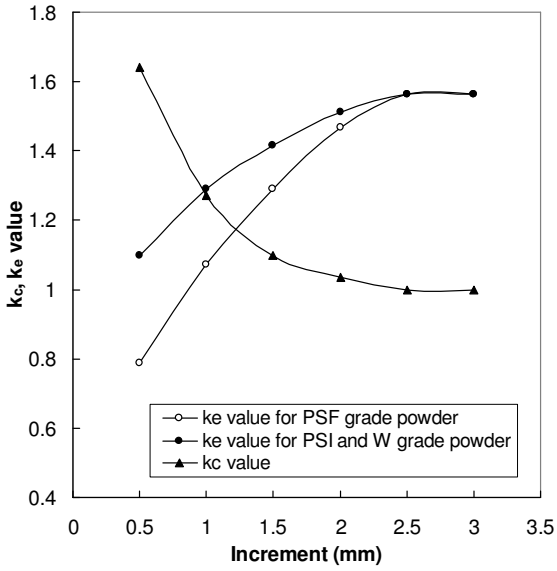

Figure 9. Effect of increment on the variation of k_c and k_e values for different powders.

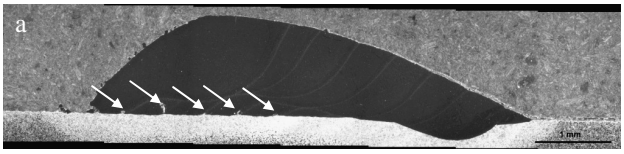

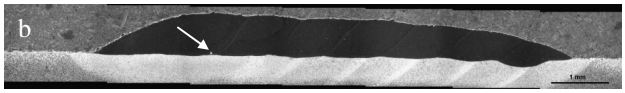

Figure 10. Appearance of inter-track porosity from the 3rd and 7th track at (a) increment of 0.5mm and (b) increment of 1 mm.

Conclusions

(1) Laser melted cross-section area increases dramatically with track number and reaches a steady value because of the heat build-up. The ratio of the steady area over the single-track area depends on the melt pool size, increment and the powder particle size. Lower heat build-up is found with finer particles and leads to lower total area and higher tendency of inter-track porosity at smaller increment.

(2) In the multi-track laser cladding, the incident laser melts not only the injected powder but also the previous track clad. The ratio of cross-section of remelted area to the total area increases with dilution and reaches a maximum value of track overlap percentage when the dilution is over 20%.

(3) Cross-section of clad area increases smoothly with the track number and reaches its steady value because of the enlarged melt pool size and enhanced laser absorption efficiency due to the changing incident angle of laser beam. The ratio of steady clad area to the single-track clad area increases with increasing track overlap.

(4) The inter-track porosity in multi-track laser cladding is produced because of decreased attenuation of laser power through the powder jet. Whether inter-track porosity forms depends not only on the aspect ratio and ratio of clad height to increment but also on the dilution in single-track clad. To achieve inter-track porosity free multi-track clad, the condition of $k < k_e$ must be observed.

References

[1] Steen, W.M., Weerasinghe, V.M., Monson, P. (1986) Some aspects of formation of laser clad tracks, in Proceedings of SPIE Vol. 650: High power laser and their industrial applications, 226-234.

[2] Weerasinghe, V.M., Steen, W.M. (1983) Laser cladding by powder injection, in Proceedings of the 1st International Conference on Lasers in Manufacturing, Brighton, UK, 125-132.

[3] Shepeleva, L., Medres, B., Kaplan, W.D., Bamberger, M., Weisheit, A. (2000) Laser cladding of turbine blade, Surface and Coatings Technology 125, 45-48.

[4] Kathuria, Y.P (2000) Some aspects of laser surface cladding in the turbine industry, Surface and Coatings Technology 132, 262-269.

[5] Peters, T., Jahnen, W. (2002). Steam turbine leading edge repair by stellite laser cladding, in Proceedings of EPRI, ST7. in CD-ROM.

[6] De Hosson, J.T.M., De Mol van Otterloo, L. (1997) Surface engineering with lasers: application to Co based materials, Surface Engineering 13, 471-481.

[7]. Sun, S., Durandet, Y., Brandt, M. (2004) Correlation between melt pool temperature and clad formation in pulsed and continuous wave Nd:YAG laser cladding of stellite 6, in Proceedings of the 1st PICALO. Melbourne, Australia, in CD-ROM.

[8] Colaco, R., Carvalho, T., Vilar, R. (1994) Laser cladding of stellite 6 on steel substrate, High Temp. Chem. Processes 3, 21-29.

[9] So, H., Chen, C.T., Chen, Y.A. (1996) Wear behaviors of laser-clad stellite alloy 6, Wear 192, 78-84.

[10] Lemoine, F., Grevey, D.F., Vannes, A.B. (1993) Cross-Section Modeling Laser Cladding, in Proceedings of the 12th ICALEO, Orlando, Florida, 1993, pp. 203-212.

[11] Chen, X., Tao, Z. (1989) Maximum thickness of the laser cladding, Key Engineering Materials 46 & 47, 381-386.

[12] Komvopoulos K. (1994) Effect of process parameters on the microstructure, geometry and microhardness of laser-clad coating materials, Mat. Sci. Forum 163-165, 417-422.

[13] Sun, S., Durandet, Y., Brandt, M (2005) Parametric investigation of pulsed Nd:YAG laser cladding of satellite 6 on stainless steel, Surface and Coatings Technology 194, 225-231.

[14] Weerasinghe, V.M., Steen, W.M. (1983) Computer simulation model for laser cladding, in Proceedings of Conference of Transport Phenomena in Material Processing, ASME, New York, 15-23.

[15] Li, Y., Ma, J. (1997) Study on overlapping in the laser cladding process, Surface and Coatings Technology 90, 1-5.

[16] Picasso, M., Marsden, C.F., Wagniere, J.-D., Frenk, A., Rappaz, M. (1994) A simple but realistic model for laser cladding, Metallurgical and Materials Transactions 25B, 281-291.

[17] Frenk, A., Vandyoussefi, M., Wagniere, J.-D., Zryd, A., Kurz, W. (1997) Analysis of the laser-cladding process for stellite on steel, Metallurgical and Materials Transactions 28B, 501-508.